Time Scale Model for the Prediction of the Onset of Flame Flashback Driven by Combustion Induced Vortex Breakdown

M. Konle
e-mail: konle@td.mw.tum.de

T. Sattelmayer

Lehrstuhl für Thermodynamik,
TU München,
Boltzmannstrasse 15,
Garching D-85748, Germany

Flame flashback driven by combustion induced vortex breakdown (CIVB) represents one of the most severe reliability problems of modern gas turbines with swirl stabilized combustors. Former experimental investigations of this topic with a 500 kW burner delivered a model for the prediction of the CIVB occurrence for moderate to high mass flow rates. This model is based on a time scale comparison. The characteristic time scales were chosen following the idea that quenching at the flame tip is the dominating effect preventing upstream flame propagation in the center of the vortex flow. Additional numerical investigations showed that the relative position of the flame regarding the recirculation zone influences the interaction of the flame and flow field. The recent analysis on turbulence and chemical reaction of data acquired with high speed measurement techniques applied during the CIVB driven flame propagation by the authors lead to the extension of the prediction model. As the corrugated flame regimes at the flame tip prevails at low to moderate mass flow rates, a more precise prediction in this range of mass flow rates is achieved using a characteristic burnout time $\tau_b \sim 1/S_l$ for the reactive volume. This paper presents first this new idea, confirms it then with numerical as well as experimental data, and extends finally the former model to a prediction tool that can be applied in the full mass flow range of swirl burners. [DOI: 10.1115/1.4000123]

1 Introduction

It has been shown in the past that the reliability of swirl stabilized lean premixed gas turbine burners can be severely limited by sudden flame flashback, which leads to overheat and severe damage within a few seconds. In former studies [1,2] combustion induced vortex breakdown (CIVB) has been identified as one possible cause. This phenomenon is characterized by an upstream propagation of the flame on the burner axis against high axial flow velocity with propagation speeds far beyond the turbulent flame speed [3]. Especially burner systems without central bluff body and purely aerodynamic stabilization are prone to CIVB, but even for burners with central obstacle flame propagation caused by CIVB can be observed [4].

The rapid flame propagation in vortex tubes driven by flame vortex interaction was the subject of different theoretical approaches [5–7]. Even though the sudden flame propagation caused by CIVB and the rapid flame propagation in vortex tubes have similarities, the CIVB phenomenon could not be described with these former concepts. With the research of Putnam and Jensen [8] and the work of Abdel-Gayed et al. [9,10], Kröner et al. [11] developed a prediction model for the occurrence of CIVB driven flame propagation.

After further investigations on the phenomenon with numerical unsteady Reynolds averaged Navier-Stokes simulations (URANS) [12] and new measurement techniques [13] established a better understanding of the dominating effects during CIVB driven flame propagation, the authors were able to extend the prediction model of Kröner et al. [11]. In Sec. 2, this paper gives a short overview of the former results, and in the following the model extension is presented. After that theoretical part, the burner geometry and the measurement techniques are shortly explained before the results of the new model obtained after its combination with the former model are shown.

2 Theory

The theoretical model for the prediction of CIVB described in this paper extends the former method of correlating CIVB limits [11] and includes the findings of numerical investigations made in parallel to the experimental investigations [12]. The physical understanding derived from both references is shortly summarized in the following. Based on the classification of the local combustion regime at the CIVB onset in the Borghi diagram [14], a model extension is then presented for the correlation of flashback limits.

2.1 Time Scale Modeling. In earlier studies, the CIVB phenomenon was investigated with a 500 kW class burner [11]. Local extinction was identified as the major effect by analyzing the temporal behavior of the flame propagation caused by CIVB. As a consequence, the occurrence of CIVB driven flame flashback was successfully correlated with a chemical time scale describing local quenching of the flame. Kröner defined a burner specific constant C_{quench}

$$C_{\text{quench}} \leq \frac{\tau_c^*}{\tau_u} = \frac{\text{Le} \cdot \tau_{\text{PSR}} \cdot \bar{u}}{D} \tag{1}$$

with which the CIVB flashback limits could be predicted over a wide range of operation. The application of Kröner's model needs some reference measurements of stability limits to define the specific constant. The prediction of flashback limits can then be realized by calculating the corresponding time scales [11]. Kröner was able to show that his model correlated the flashback limits measured for higher Re numbers very well. In this range, the effects of air preheat and of fuel composition were well captured. However, systematic deviations of the data from the model predictions were also observed. With the model extension presented below the observed limitations are overcome.

Contributed by International Gas Turbine Institute (IGTI) of ASME for publication in the JOURNAL OF ENGINEERING FOR GAS TURBINES AND POWER. Manuscript received April 9, 2009; final manuscript received April 14, 2009; published online January 27, 2010. Editor: Dilip R. Ballal.

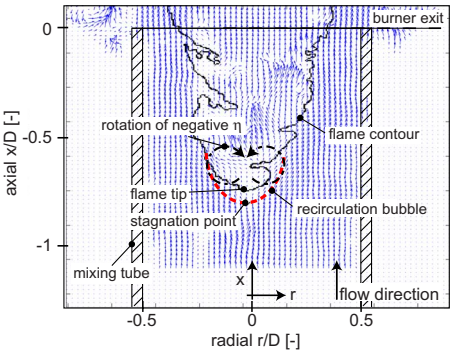

Fig. 1 Instantaneous image of the propagating bubble and flame: the reaction layer is only moderately corrugated [13]

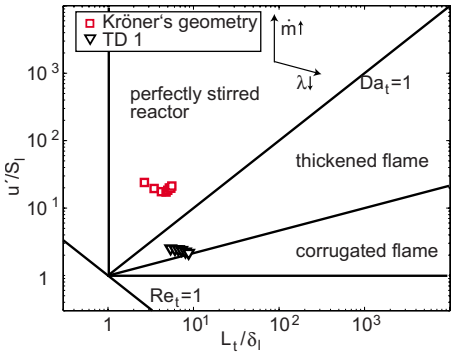

Fig. 2 Burning regime in the core flow of the investigated burners in the Borghi diagram

2.2 Combustion Induced Vortex Breakdown. The significance of chemistry-turbulence interaction for CIVB was analyzed numerically by Kiesewetter et al. [12]. After successful mapping of the flow on two dimensions, he used axisymmetric URANS to compute CIVB. In these computations the equivalence ratio was gradually increased until the flame propagated through the mixing tube following the tip of a recirculation bubble (i.e., its stagnation point, see Fig. 1) appearing in the flame tube first. The vorticity transport equation [15] was used to analyze the interaction of the flow field and the reaction neglecting the diffusion and dissipation terms because of their minor importance, as suggested by Hasegawa et al. [16], as follows:

$$\frac{D\boldsymbol{\omega}}{Dt} = \frac{\partial}{\partial t}\boldsymbol{\omega} + (\boldsymbol{U}\cdot\nabla)\boldsymbol{\omega} = (\boldsymbol{\omega}\cdot\nabla)\boldsymbol{U} - \boldsymbol{\omega}(\nabla\cdot\boldsymbol{U}) + \frac{1}{\rho^2}(\nabla\rho\times\nabla p) \tag{2}$$

Chemical reaction leads to two contributions to the vorticity budget—the volume expansion (second term on the rhs) and the baroclinic torque (third term on the rhs)—which influence the equilibrium of the axial flow U_{axial} and the upstream flow u_{ind} induced by the azimuthal vorticity component η according to the law of Biot–Savart [17]

$$u_{\text{ind}}(x) = \frac{1}{2}\int_{-\infty}^{\infty}\int_{0}^{\infty}\frac{r^{*2}\eta(r^*,x^*)}{[r^{*2}+(x-x^*)^2]^{3/2}}dr^*dx^* \tag{3}$$

As this equation shows, only negative azimuthal vorticity η leads to an upstream directed flow. The postprocessing of the URANS data finally delivered the root cause of CIVB: While the contribution of the volume expansion to the change in azimuthal vorticity is positive and thus stabilizes the flow field, the negative contribution of the baroclinic torque stimulates the upstream propagation of the flame. The competitive character of these two terms explains the importance of the relative position of the flame regarding the recirculation bubble found in the numerical studies: The flame position must provide favorable conditions for the generation of high negative vorticity to induce the formation and the propagation of a closed recirculation bubble that serves as flame holder. In the stable range, the partial compensation of the negative vorticity by the volume expansion inhibits flame flashback.

2.3 Prediction Model Extension. Using time scale modeling, Kröner showed that the onset of CIVB driven flame propagation can be correlated with two characteristic time scales τ_u and τ_{PSR}. The correlation law according to Eq. (1) is based on the experiences collected with the burner investigated in Kröner's studies, operated with high volumetric flow [11] characteristic for gas turbine burners. However, the underlying assumption that the closed recirculation bubble can be interpreted as a perfectly stirred reactor (PSR) is not always strictly valid in the entire operation field of a burner. In contrast to the idea of a perfectly stirred flame zone in the propagating bubble, Kiesewetter et al. [12] computed a combustion regime with a well defined flame surface. Although this finding is mainly due to the fairly simple combustion model he applied and does not fully represent reality in the high velocity regime, it was verified with experimental results obtained by the authors [13] for a swirl burner with lower turbulent Re numbers and lower mass flow rates as well as a larger vortex core than for the design investigated by Kröner. Figure 1 shows an instantaneous image of a propagating flame for this new geometry. During sudden upstream propagation the dynamic evolution of the flame front was detected via laser induced fluorescence (LIF) and the flow field with particle imaging velocimetry (PIV). The flame is following the upstream propagating recirculation bubble (the dotted line illustrates the bubble contour in Fig. 1) with a substantial spatial separation. The surface of the reaction zone inside the bubble is only moderately corrugated. No evidence of massive flame thickening in the bubble was found in these experiments and thus the stirred reaction zone in the bubble postulated by Kröner was not observed for the present operating conditions. In Sec. 3 this study investigates this new burner (*TD1 burner*) operated at low flow rates in more detail to achieve a correlation law for low turbulent Re numbers before a general correlation model for the prediction of CIVB driven flame flashback is defined by coupling the experiences made with both burners, which cover a wide range of pressure drops and volumetric flow velocities.

To classify the reaction zone for the TD1 burner the local burning conditions inside the recirculation bubble were classified using the Borghi diagram in its classical form [14]. Since the increase in mass flow increases also the turbulent fluctuation (u'), the variation in mass flow generally represents a vertical shift inside the Borghi diagram under the assumption of an almost constant L_t that is mainly predominated by the geometry of the mixing tube [18]. Changes in the air excess ratio λ lead to changes in the laminar flame speed S_l as well as the flame thickness δ_l and thus to a diagonal shift in the Borghi diagram.

In the Borghi diagram shown in Fig. 2, the flame regime representative for the combustion in the bubble is plotted for the TD1 burner as well as for the burner investigated by Kröner. The values of u' inside the recirculation bubble as well as the integral length scale L_t inside the mixing tube were estimated with laser optical measurement techniques. The flame thickness δ_l and laminar flame speed S_l were quantified with correlations published in the literature (see Refs. [19,20], respectively). In particular for high mass flows, the burner geometry investigated by Kröner has high local turbulence inside the recirculation bubble and the stirred regime is well suitable to characterize the reaction-turbulence interaction for this burner. However, the local interaction of chemistry and flow inside the recirculation bubble is better represented by the corrugated flame regimes for the TD1 burner observed at the volumetric flow velocities covered in the study. Because of the different burning regimes in the core flow, gener-

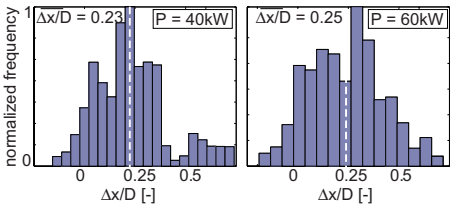

Fig. 3 Distribution of the instantaneous axial distance between the stagnation point of the recirculation bubble and flame tip for two operation points

ally applicable correlation laws have to take into account the actually present burning regime, which is substantially influenced by the mass flow rate.

For the TD1 burner the authors previously published a simultaneous analysis of reaction and flow field during CIVB driven flame propagation with high temporal resolution [3]. Figure 3 shows for two operation points the distribution of the measured spatial separation between the stagnation point of the recirculation bubble and the flame tip. The data were taken from simultaneous PIV/LIF measurements during CIVB driven flame propagation. The number of samples was limited due to the limited observation time [3]. Nevertheless, the limited database revealed clearly that the median value for the spatial separation of the stagnation point and flame tip is about 0.25 D independent of the mass flow rate. Since additional data for other thermal power confirmed this observation, the conclusion was made that the critical spatial separation Δx_{crit} for the onset of CIVB driven flame propagation remains almost constant and independent of the volumetric flow velocity. This experimental observation confirms the importance of the spatial deviation of flame and bubble as explained before with the vorticity transport equation (Eq. (2)): Independent of the mass flow rate the critical distance Δx_{crit} (Fig. 4) represents the relative flame position regarding the bubble, which provides favorable conditions for the production of high negative azimuthal vorticity η to induce sudden upstream propagation [12].

Because of these observations, the missing correlation law for the onset of CIVB for low to moderate turbulent Re numbers has to correspond to the experimental finding that the reactive fluid in the bubble is consumed by a corrugated flame. Since the radial dimension of the bubble correlates with the burner diameter and its shape is almost independent of the flow velocity, the volume of the reactive mixture in the bubble is predominantly governed by the spatial separation of the stagnation point and flame tip.

Figures 4(a) and 4(b) illustrate this idea for a stable operation point without flame propagation and for the onset of CIVB driven flame propagation, respectively. The important difference is the spatial separation of the stagnation point and flame tip: For stable conditions the distance Δx has not yet dropped to the critical

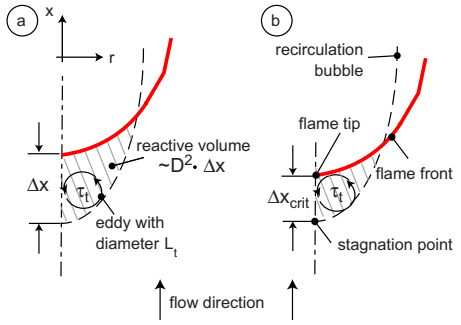

Fig. 4 Principle of the prediction model extension: invariant reactive volume between corrugated flame front and bubble contour at the onset of CIVB

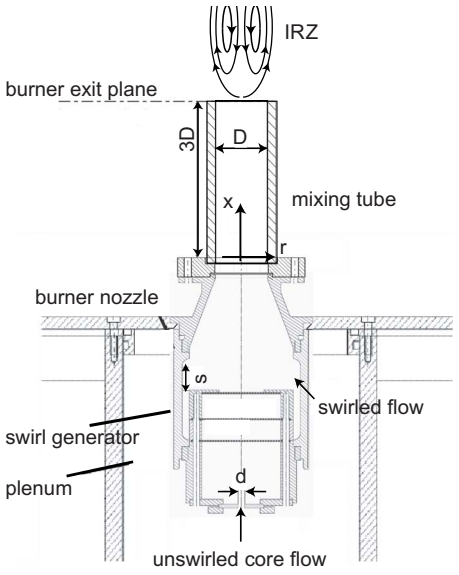

Fig. 5 Scheme of the investigated TD1 burner

distance. For this reason the relative position of the flame regarding the recirculation bubble does not yet produce conditions favorable enough for the onset of CIVB because the net production of negative azimuthal vorticity is insufficient to initiate flame propagation [12].

These observations lead to the following equations for the characteristic turbulent time scale τ_t and the characteristic time scale for the burnout of the reactive volume τ_b:

$$\tau_t = \frac{L_t}{u'} \sim \frac{D}{\bar{u}} \tag{4}$$

$$\tau_b = \frac{\Delta x_{\text{crit}}}{S_t} \sim \frac{\Delta x_{\text{crit}}}{S_l} \tag{5}$$

The fact that the flame inside the bubble exhibits a smooth and moderately wrinkled surface and the finding that the reaction inside the bubble is of weak turbulence allows the conclusion $S_t \sim S_l$, which is based on the early work of Damköhler [21]. As Kröner did for his correlation law (Eq. (1)), these two characteristic time scales are compared with each other and the ratio is used to define a characteristic constant C_b as follows:

$$\frac{\tau_b}{\tau_t} \sim \frac{\Delta x_{\text{crit}} \cdot \bar{u}}{S_l \cdot D} = C_b \tag{6}$$

This correlation can further be simplified, introducing the constant ratio of Δx_{crit} and D. Finally, this leads to the simple result that the ratio of bulk velocity and laminar flame speed has to be a constant for all operation points near the onset of CIVB. Thus, the experimental determination of this ratio via at least one reference measurement allows the prediction of CIVB driven flame flashback for the entire operation range. The ratio of both time scales can be interpreted as the balance between the turbulent time for the rotation of an eddy of the integral length scale L_t and the chemical time for the laminar burnout of the reactive volume inside the unburned recirculation zone (Fig. 4).

3 Experimental Setup

3.1 Test Rig. The burner configuration used for this study (TD1 burner) was derived from the swirler design published in Ref. [22]. This burner applies aerodynamical flame stabilization without bluff body on the center line. The stabilization of the reaction is achieved with an internal recirculation zone (IRZ) at the burner exit (Fig. 5). The tangential inlet ports for the main air

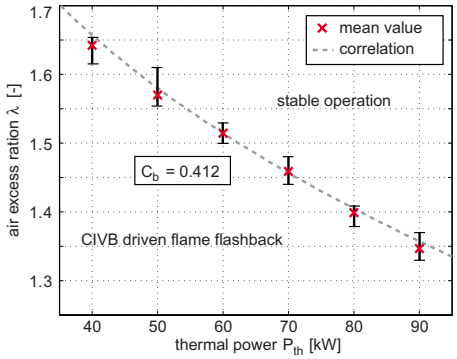

Fig. 6 Experimental CIVB limits and prediction for the TD1 burner with *s*=22 mm and *d*=12 mm

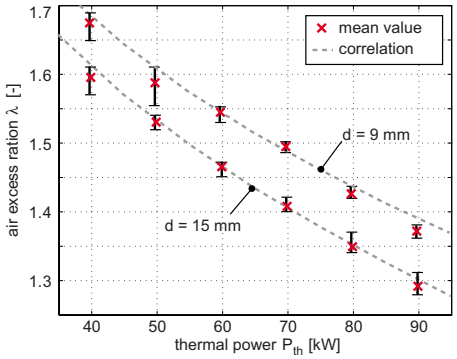

Fig. 7 Experimental CIVB limits and prediction for variation in the axial inlet diameter (configurations: *d*=9 mm and *d* =15 mm)

provide the swirl required for the breakdown of the flow downstream of the mixing tube. Variation in the open slot length s changes the swirl level. An additional axial jet is added on the burner axis for tailoring the velocity field. With the variation in the axial inlet diameter d, the vortex core radius of the flow can be varied. More details on the influence of the geometric parameters (burner diameter D, open slot length s, and axial inlet diameter d) are given in Ref. [3]. The flame propagation from the combustion chamber into the swirl generator can be observed using a silica glass cylinder serving as the mixing tube.

3.2 Measurement Techniques. The combination of two measurement techniques with high temporal resolution were used for the investigation of the chemistry-turbulence interaction: The flow field analysis was carried out with a PIV system composed of a Photron APX high speed camera and a dual cavity Nd:YLF laser with an emitted wavelength of 527 nm. The temporal resolution was set to 1000 Hz, the upper limit given by the maximum repetition rate of the simultaneously applied LIF system. This LIF system, which is used for the detection of the flame front, excited the OH radical with a wavelength of 282.925 nm. The sudden increase in the combustion intermediate concentration indicates the reaction zone and thus the flame front [23]. The simultaneous use of the high speed measurement techniques PIV and LIF, for the first time published in Ref. [24], required a complex data postprocessing because of reflections stemming from the glass confinement and from the deposition of seeding particles during the tests. More detail of the measurement systems and the data postprocessing are given in Ref. [3].

3.3 Experimental Method. In principle CIVB driven flame propagation can be initiated either by the reduction in the air excess ratio λ or by the reduction in the mass flow rate [11]. In this study the first procedure was chosen. After ignition of the burner under lean conditions ($\lambda \approx 2.0$), CIVB driven flame propagation was initiated by reducing λ with a temporal gradient of about $\Delta\lambda/\Delta t = 0.01\ s^{-1}$. For the determination of the critical air excess ratio λ_{crit}, every operation point was measured ten times to calculate an average value of the critical λ-value. The maximum deviation to its average value was less than $\Delta\lambda = 0.05$ (see error bars in Fig. 6).

4 Results

As already mentioned, the scaling law for the prediction of flame flashback driven by combustion induced vortex breakdown published by Kröner et al. [2] was based on the investigation of one burner geometry. Figure 2 shows that the burning conditions on the axis of swirl stabilized burners are not always strictly represented by the stirred reaction regime and that at moderate mass flow rates, the local reaction is better represented by the corrugated flame regime. This section first presents the flashback limits of the TD1 burner operated at low to moderate mass flow rates before the prediction model extension is coupled with the former model and used to correlate the CIVB limits of the geometry investigated by Kröner et al. [11].

4.1 Prediction of the Onset of CIVB. The CIVB limits for the TD1 burner (D=40 mm burner diameter, s=22 mm open slot length, and d=12 mm axial inlet diameter, see Fig. 5 and Refs. [3,13] for details) are plotted in Fig. 6. For this geometry a characteristic constant $C_b = 0.412$ according to Eq. (6) was determined using the critical operation point $P_{th} = 60$ kW and $\lambda_{crit} = 1.52$ as the reference. Since the new approach correlates the flashback limits with the reciprocal value of the laminar flame speed instead of its square according to the classical definition of $\tau_c = a/S_l^2$, the values for C_b are one order of magnitude larger than the C_{quench} constant (Eq. (1)).

Using the mentioned constant $C_b = 0.412$, the critical values of λ were then predicted for the entire operation range of the investigated burner by calculating the corresponding time scales. The predicted flashback limits are plotted in Fig. 6 with the dotted line. This prediction is in good agreement with the experimental data (the markers in Fig. 6 show the mean values). The main reason for this behavior is that combustion in the bubble takes place in a flame front, which is directly represented by the laminar propagation speed. Over the entire operation range of the TD1 burner shown in Fig. 6 the assumption of a corrugated flame regime in the bubble remains valid (Fig. 2).

The variation in the axial inlet diameter d leads to a variation in the core radius of the swirling flow [3] and changes the geometry specific constant. Figure 7 shows the analysis for two other vortex core diameters generated with axial inlet diameters of d=9 mm and d=15 mm (Fig. 5). The estimated constant C_b was 0.452 for d=9 mm and 0.352 for d=15 mm, again determined with the critical value at P_{th}=60 kW thermal power. The lower value for the larger diameter indicates better flashback resistance. As shown before for the diameter of d=12 mm (Fig. 6), the correlation law (Eq. (6)) also holds for these flashback experiments independent of the particular choice of the diameter of the axial inlet (Fig. 7). The maximum deviation between the predicted air excess ratio λ and the measured λ is less than 0.025. These findings allow the conclusion that the flashback limits can be successfully correlated with the new model for flows with different vortex core radii.

The new model was tested with respect to its applicability for the prediction of CIVB limits for preheated mass flows as well. Figure 8 shows, for three fuel mass flow rates of the TD1 burner, the air excess ratio limits with increasing mixture temperature in the range of 300–420 K covered in the study. Obviously, the critical air excess ratio increases with increasing inlet temperature. This behavior was previously reported by Kröner for his geometry and he also modeled the effect with his time scale comparison.

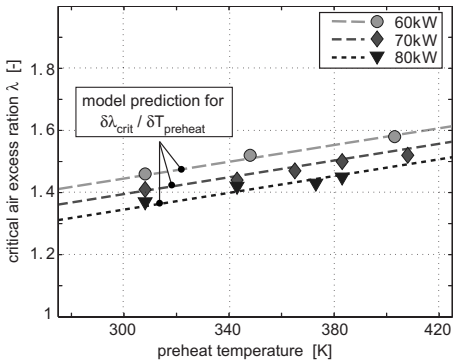

Fig. 8 Influence of the preheat temperature on the CIVB limits and prediction

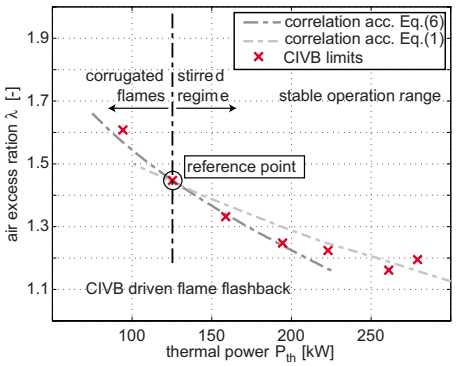

Fig. 9 Experimental CIVB limits and prediction for the burner geometry investigated by Kröner et al. [11] with the coupled correlation laws

The temperature increase influences the laminar flame speed S_l and the bulk velocity $\bar{u}$ via the density decrease. The correlation law (Eq. (6)) delivers the gradients $\partial\lambda_{crit}/\partial T_{preheat}$ plotted in Fig. 8. An adaptation of the estimated constant C_b is not required, and the correlation law according to Eq. (6) can properly deal with changes in the mixture temperature. The model prediction and the experimental results are in good agreement.

In summary, the detailed analysis of the TD1 burner shows the applicability of the new correlation law for the corrugated flame regime. The missing final step toward a universally applicable model covering both flame regimes is the combination of this approach with the former model of Kröner et al. [11].

4.2 Coupled Prediction Model. The combination of both models is based on the proper choice of the chemical time scale: For all operation conditions with corrugated flames, the newly defined correlation can be used. For higher mass flow rates the higher turbulence changes the combustion toward the *stirred reactor* regime and, thus, the PSR time scale is better suited for a correct prediction. In this operation range the reaction-turbulence interaction is strongly dominated by turbulent quenching. The assumption of a corrugated flame in the bubble is not valid anymore and the reactive volume approaches the stirred reactor regime.

For the TD1 burner no change in the local combustion regime (Fig. 2) occurs within the investigated power range and the correlation law for the corrugated flame regimes (Eq. (6)) is well suited in the entire operation range of this burner for the calculation of the onset of CIVB. However, as the burner geometry investigated by Kröner et al. [11] was tested in a very wide range, the change in the local burning conditions in the bubble with increasing mass flow rate from the corrugated flame regimes to the stirred regime has to be taken into account. Consequently, the coupling of the two approaches (Eqs. (6) and (1)) is required for the prediction of the CIVB onset with high accuracy in the entire operation range.

The simultaneous use of the chemical time scales τ_b and τ_{PSR} for the geometry investigated by Kröner is plotted in Fig. 9. The critical operation point $P_{th}=125$ kW and $\lambda_{crit}=1.44$ is the reference point used for the estimation of the geometry specific constants $C_b=0.153$ and $C_{quench}=0.030$ [11]. The two curves show the correlation laws according to Eq. (6) and Eq. (1), respectively. For stable operation, the burner has to be operated above the critical air excess ratios predicted by both correlation laws. The validity for Eqs. (6) and (1) ends at the intersection of the curves: For low to moderate mass flow rates, the assumption of corrugated flames is obviously also valid for the burner investigated by Kröner et al. [11] and predicts the limits for the onset of CIVB very well. With increasing mass flow rates the model of Kröner et al. [11] is better suited for the prediction. The combined use of both time scales allows the precise prediction over the entire operation range of the burner. The maximum deviation between the modeled λ_{crit} and the measured λ_{crit} is smaller than 0.025.

In summary, the combination of the two correlation laws (Eqs. (1) and (6)) to an extended model allows to predict CIVB limits in the development stadium of premix burners by determination of the burner specific constants C_{quench} and C_b with a low number of experiments and the determination of the burning conditions in the center of the swirling flow via the Borghi diagram, which delivers the prevailing combustion regime. The constants C_b and C_{quench} are linked to each other at the point of intersection of both prediction curves. Considering the point of intersection (PI) and Eqs. (1) and (6), the ratio between C_b and C_{quench} is given by

$$\frac{C_b}{C_{quench}} = \left.\frac{\Delta x_{crit}}{S_l \cdot \tau_{PSR}}\right|_{PI} \tag{7}$$

5 Conclusions and Outlook

Sudden flame propagation driven by CIVB is a severe problem for the reliability of premixed swirl burners. Detailed former studies of CIVB [11,12] delivered a model for the prediction of the onset of CIVB driven flame propagation for high turbulent Re numbers. A model for moderate turbulent Re numbers was developed in this study and combined with the former one.

The approach is the classification of the burning regime at the flame tip in the Borghi diagram: For low turbulent Reynolds numbers and low to moderate mass flow rates, the small influence of turbulence on the reaction corresponds to the corrugated flame regime. The chemical time scale best suited for this regime to predict the onset of CIVB driven flame propagation is proportional to $1/S_l$. At higher mass flow rates, the influence of turbulence becomes significant and the burning conditions inside the recirculation bubble correspond to the stirred regime. The appropriate characteristic time scale for this regime is τ_{PSR}. Both chemical time scales compared with characteristic flow time scales deliver a correlation law for each regime. A prediction model for the onset of CIVB driven flame propagation with high accuracy over the entire operation range of the test burners was achieved by the combination of these two correlation laws.

Without knowledge of the location of the intersection point in the specific design case, additional work is required for the determination of a second constant. This may be seen as a drawback concerning the applicability of the extended model. For this reason, further investigations incorporating preheat temperature and fuel composition will be made to find a rule for the change in the reaction regime for turbulent aerodynamically stabilized flames. Upon the experimental determination of one of both constants, this rule will allow the direct calculation of the second burner constant according to Eq. (7) and thus reduce the required number of reference measurements.

Acknowledgment

The authors gratefully acknowledge the financial support provided by the German Research Council (DFG).

Nomenclature

a = thermal diffusivity (m^2/s)
C_b = burnout constant
C_{quench} = quenching constant
D = burner diameter (m)
Le = Lewis number
L_t = integral length scale (m)
P_{th} = thermal power (kW)
p = pressure (bar)
Re = Reynolds number
S_l = laminar flame speed (m/s)
S_t = turbulent flame speed (m/s)
r = radial coordinate (m)
t = time (s)
$\boldsymbol{U}$ = velocity vector (m/s)
$\bar{u}$ = bulk velocity (m/s)
u_{ind} = axial upstream velocity induced by η (m/s)
x = axial coordinate, flow direction (m)
Δx = spatial deviation (m)
δ_l = flame thickness (m)
η = azimuthal component of $\boldsymbol{\omega}$ (1/s)
ρ = density (kg/m^3)
τ_b = characteristic time scale for burnout (s)
τ_c = chemical time scale (s)
τ_{PSR} = chemical time scale for PSR (s)
τ_t = turbulent time scale (s)
τ_u = characteristic flow time scale (s)
$\boldsymbol{\omega}$ = vorticity vector (1/s)

References

[1] Fritz, J., Kröner, M., and Sattelmayer, T., 2001, "Flashback in a Swirl Burner With Cylindrical Premixing Zone," *Proceedings of the ASME Turbo Expo*, LA.
[2] Kröner, M., Fritz, J., and Sattelmayer, T., 2002, "Flashback Limits for Combustion Induced Vortex Breakdown in a Swirl Burner," *Proceedings of the ASME Turbo Expo*, The Netherlands.
[3] Konle, M., and Sattelmayer, T., 2008, "Interaction of Heat Release and Vortex Breakdown in Swirling Flames," *Proceedings of the 14th International Symposium on Applications of Laser Techniques to Fluid Mechanics*, Portugal.
[4] Noble, D. R., Zhang, Q., Shareef, A., Tootle, J., Meyers, A., and Lieuwen, T., 2006, "Syngas Mixture Composition Effects Upon Flashback and Blowout," *Proceedings of the ASME Turbo Expo*, Spain.
[5] McCormack, P. D., Scheller, K., Mueller, G., and Tisher, R., 1972, "Flame Propagation in a Vortex Core," Combust. Flame, **19**, pp. 297–303.
[6] Asato, K., Wada, H., Hiruma, T., and Takeuchi, Y., 1997, "Characteristics of Flame Propagation in a Vortex Core: Validity of a Model for Flame Propagation," Combust. Flame, **110**, pp. 418–428.
[7] Umemura, A., and Tomita, K., 2001, "Rapid Flame Propagation in a Vortex Tube in Perspective of Vortex Breakdown Phenomena," Combust. Flame, **125**, pp. 820–838.
[8] Putnam, A. A., and Jensen, R. A., 1948, "Application of Dimensionless Numbers to Flashback and Other Combustion Phenomena," Third International Symposium on Combustion, Flame and Explosion Phenomena, pp. 89–98.
[9] Abdel-Gayed, R. G., and Bradley, D., 1985, "Criteria for Turbulent Propagation Limits of Premixed Flames," Combust. Flame, **62**, pp. 61–68.
[10] Abdel-Gayed, R. G., Bradley, D., and Lung, F. K. K., 1989, "Combustion Regimes and the Straining of Turbulent Premixed Flames," Combust. Flame, **76**, pp. 213–218.
[11] Kröner, M., Sattelmayer, T., Fritz, J., Kiesewetter, F., and Hirsch, C., 2007, "Flame Propagation in Swirling Flows—Effect of Local Extinction on the Combustion Induced Vortex Breakdown," Combust. Sci. Technol., **179**, pp. 1385–1416.
[12] Kiesewetter, F., Konle, M., and Sattelmayer, T., 2007, "Analysis of Combustion Induced Vortex Breakdown Driven Flame Flashback in a Premix Burner With Cylindrical Mixing Zone," ASME J. Eng. Gas Turbines Power, **129**, pp. 929–936.
[13] Konle, M., Kiesewetter, F., and Sattelmayer, T., 2008, "Simultaneous High Repetition Rate PIV-LIF-Measurements of CIVB Driven Flashback," Exp. Fluids, **44**, pp. 529–538.
[14] Borghi, R., 1988, "Turbulent Combustion Modelling," Prog. Energy Combust. Sci., **14**, pp. 245–292.
[15] Darmofal, D. L., 1993, "The Role of Vorticity Dynamics in Vortex Breakdown," AIAA Paper No. 93-3036.
[16] Hasegawa, T., Nishiki, S., and Michikami, S., 2001, "Mechanism of Flame Propagation Along a Vortex Tube," *IUTAM Symposium on Geometry and Statistics of Turbulence*, Kluwer, Dordrecht, The Netherlands, pp. 235–240.
[17] Panton, R. L., 1996, *Incompressible Flow*, Wiley, New York.
[18] Hoffmann, S., Habisreuther, P., and Lenze, B., 1994, "Development and Assessment of Correlations for Predicting Stability Limits of Swirling Flames," Chem. Eng. Process., **33**, pp. 393–400.
[19] Turns, S. R., 2000, *An Introduction to Combustion*, 2nd ed., McGraw-Hill, New York.
[20] Peters, N., 1994, "Turbulente Brenngeschwindigkeit," Abschlussbericht zum Forschungsvorhaben, Report No. Pe 241/9-2.
[21] Damköhler, G., 1940, "Der Einfluss der Turbulenz auf die Flammengeschwindigkeit in Gasgemischen," Z. Elektrochem. Angew. Phys. Chem., **46**, pp. 601–626.
[22] Burmberger, S., Hirsch, C., and Sattelmayer, T., 2006, "Designing a Radial Swirler Vortex Breakdown Burner," *Proceedings of the ASME Turbo Expo*, Spain.
[23] Eckbreth, A. C., 1996, "*Laser Diagnostics for Common Combustion Temperature and Species*," *Combustion Science and Technology Book Series*, Vol. 3, Taylor & Francis, London.
[24] Konle, M., Winkler, A., Kiesewetter, F., Wäsle, J., and Sattelmayer, T., 2006, "CIVB Flashback Analysis With Simultaneous and Time Resolved PIV-LIF Measurements," *Proceedings of the 13th International Symposium on Applications of Laser Techniques to Fluid Mechanics*, Portugal.